Inorganic Chemistry

ARTICLE

pubs.acs.org/IC

Ce(IV) Complexes with Donor-Functionalized Alkoxide Ligands: Improved Precursors for Chemical Vapor Deposition of CeO_2

Helen C. Aspinall,* John Bacsa, Anthony C. Jones, and Jacqueline S. Wrench

Department of Chemistry, Donnan and Robert Robinson Laboratories, University of Liverpool, Crown Street, Liverpool, L69 7ZD, U.K.

Kate Black, Paul R. Chalker, Peter J. King, Paul Marshall, and Matthew Werner

Department of Engineering, George Holt Building, University of Liverpool, Liverpool, L69 3GH, U.K.

Hywel O. Davies and Rajesh Odedra

SAFC Hitech, Power Road, Bromborough, Wirral, CH62 3QF, U.K.

Supporting Information

ABSTRACT: Thin films of ceria (CeO_2) have many applications, and their synthesis by liquid-injection MOCVD (metal−organic chemical vapor deposition) or ALD (atomic layer deposition) requires volatile precursor compounds. Here we report the synthesis of a series of homoleptic and heteroleptic Ce(IV) complexes with donor-functionalized alkoxide ligands mmp (1-methoxy-2-methylpropan-2-olate), dmap (1-(dimethylamino)propan-2-olate), and dmop (2-(4,4-dimethyl-4,5-dihydrooxazol-2-yl)propan-2-olate) and their potential as precursors for MOCVD and ALD of CeO_2. New complexes were synthesized by alcohol exchange reactions with $[Ce(OBu^t)_4]$. $[Ce(mmp)_4]$ and $[Ce(dmap)_4]$ were both found to be excellent precursors for liquid-injection MOCVD of CeO_2, depositing high purity thin films with very low carbon contamination, and both have a large temperature window for diffusion controlled growth (350−600 °C for $[Ce(mmp)_4]$; 300−600 °C for $[Ce(dmap)_4]$). $[Ce(mmp)_4]$ is also an excellent precursor for liquid-injection ALD of CeO_2 using H_2O as oxygen source and demonstrates self-limiting growth from 150 to 350 °C. $[Ce(dmap)_4]$ has lower thermal stability than $[Ce(mmp)_4]$ and does not show self-limiting growth in ALD. Heteroleptic complexes show a tendency to undergo ligand redistribution reactions to form mixtures in solution and are unsuitable as precursors for liquid-injection CVD.

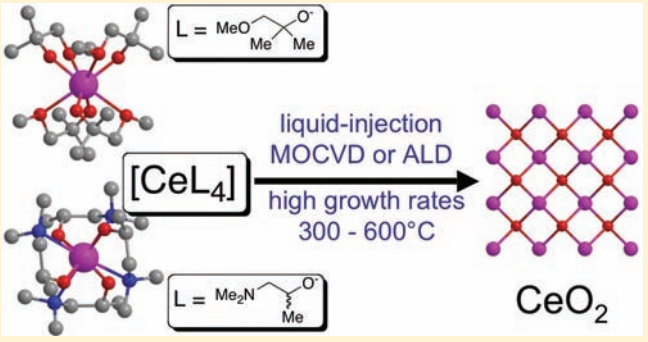

INTRODUCTION

Thin films of CeO_2 have many applications: e.g. as a dielectric in complementary metal oxide semiconductor (CMOS) and memory applications;[1] as a dopant to stabilize high-κ phases of HfO_2;[2] in magneto-optical devices;[3] in sensors;[4] as an anode material in solid oxide fuel cells.[5] MOCVD (metal−organic chemical vapor deposition) and ALD (atomic layer deposition) are important techniques for the preparation of oxide thin films,[6,7] and both of these techniques require volatile precursor compounds. $[Ce(thd)_4]$ (thd =2,2,6,6-tetramethylheptane-3,5-dionate) is probably the most widely used precursor for CVD of CeO_2. It is air- and moisture-stable, reasonably volatile, easy to synthesize, and has high thermal stability. Although these properties mean that it is quite easy to handle, they also mean that it is a less than ideal precursor for CVD. Alkoxide complexes are more attractive as CVD precursors: they have lower thermal stability than β-diketonates and hence lower deposition temperatures in MOCVD, and they are powerful Brønsted bases, meaning that they react readily with H_2O, which is a real advantage in ALD. Facile reaction of a precursor with H_2O means that H_2O can be used as an oxygen source for ALD of oxide materials: this is experimentally preferable to use of more aggressive oxygen sources such as ozone. The Ce(IV) alkoxide $[Ce(OCMe_2Pr^i)_4]$ has been investigated as a precursor for MOCVD of CeO_2,[8] but there have been no subsequent reports of its use, and we found that it had a very narrow temperature window for diffusion-controlled growth (see Results and Discussion). We therefore identified a need for more effective precursors for CeO_2, and in this paper, we report on a series of Ce(IV) alkoxides and their use for liquid-injection MOCVD and ALD of CeO_2.

It is apparent that Ce complexes with monodentate alkoxide ligands are less than ideal as CVD precursors, and so we chose to work with bidentate donor-functionalized alkoxide ligands derived from the alcohols shown in Chart 1 below.

Received: July 25, 2011
Published: October 21, 2011

Chart 1. Structures of Donor Functionalized Alcohols

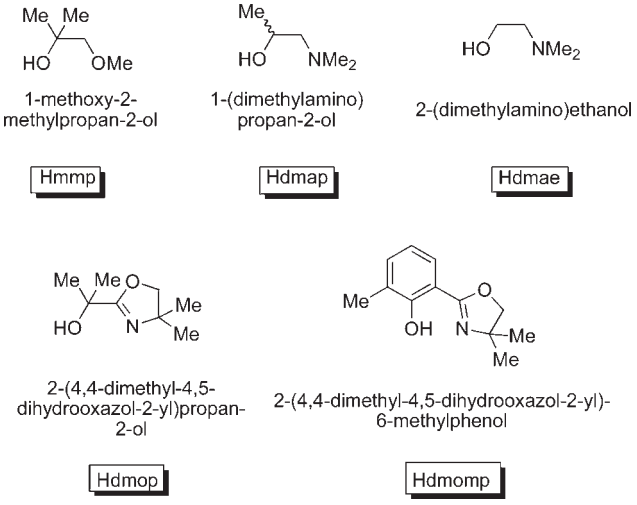

These ligands (apart from dmomp) have all been used successfully with other metals as precursors for CVD of oxides,[9,10] and we have already published a preliminary communication on the use of $[Ce(mmp)_4]$ for MOCVD of CeO_2.[11]

EXPERIMENTAL SECTION

General. Hmmp, $[NH_4]_2[Ce(NO_3)_6]$ (CAN) and $[Ce(thd)_4]$ were supplied by SAFC Hitech. Hdmop[12] and Hdmomp[13] were synthesized by the published routes. Other starting materials were purchased from Aldrich.

The preparation of all cerium complexes was performed under strictly anaerobic and anhydrous conditions using standard Schlenk techniques. Nondeuterated solvents were distilled from sodium/benzophenone ketyl and stored under N_2 over activated 4 Å molecular sieves prior to use. Deuterated solvents were distilled from CaH_2 prior to use. NMR spectra were recorded on a Bruker Avance 400 spectrometer. NMR samples of cerium complexes were sealed under vacuum. Mass spectra were recorded on a Finnigan MAT 95 XP instrument (EI and CI) by the EPSRC National Mass Spectrometry Service at Swansea University. Elemental analyses were performed by Mr. Stephen Boyer of the School of Health Sciences, London Metropolitan University.

Synthesis of Complexes. *[Ce(mmp)$_4$]* ***1***. A solution of $[NH_4]_2[Ce(NO_3)_6]$ (10.00 g, 18.24 mmol) in dimethoxyethane (DME) (77 mL) was added at room temperature to a stirred solution of $NaOBu^t$ (10.52 g, 109.4 mmol) in DME. After removal of the $NaNO_3$ precipitate, the filtrate was stirred at 0 °C and Hmmp (8.52 mL, 73.0 mmol) was added. The reaction mixture was heated under reflux for 1 h and then left to cool to room temperature. Volatiles were removed in vacuo, and the resulting yellow oil was extracted with hexane (3 × 100 mL), which was then concentrated to give the product as yellow crystals on cooling to −18 °C. (5.24 g, 52% yield).

M.p.: 105−106 °C (0.8 Torr). ^{1}H NMR (400 MHz, C_7D_8): δ(ppm): 1.27 (6H, s $OC(CH_3)_2CH_2OCH_3$), 3.60 (2H, s, $OC(CH_3)_2CH_2OCH_3$), 3.49 [3H, s, $OC(CH_3)_2CH_2OCH_3$). ^{13}C NMR (100 MHz, C_7D_8): δ(ppm): 26.9 ($OC(CH_3)_2CH_2OCH_3$), 58.2 ($OC(CH_3)_2CH_2OCH_3$), 75.0 ($OC(CH_3)_2CH_2OCH_3$), 84.1 ($OC(CH_3)_2CH_2OCH_3$). Calcd. for $CeC_{20}H_{44}O_8$: C, 43.46 ; H, 8.02; found: C, 42.58; H, 7.88%.

[Ce(dmae)$_4$] ***2*** was synthesized following the route used for $[Ce(mmp)_4]$ using CAN (1.00 g, 1.82 mmol), $NaOBu^t$ (1.05 g, 96.1 mmol), and dmaeH (0.75 mL, 7.3 mmol). The reaction mixture was refluxed for 2 h and volatiles removed in vacuo to give a yellow oil. Yield: 350 mg (39%).

Calcd for $CeC_{16}H_{40}O_4N_4$: C 39.01, H 8.18, N 11.37; found C, 38.88, H 8.08, N 11.19%. A ^{1}H NMR spectrum is shown in Figure S2 of the Supporting Information.

[Ce(dmap)$_4$] ***3*** was synthesized following the route used for $[Ce(mmp)_4]$ using CAN (7.00 g, 12.8 mmol), $NaOBu^t$ (7.36 g, 76.6 mmol), and dmapH (6.30 mL, 51.1 mmol). Recrystallization from toluene gave the complex as yellow crystals. Yield: 3.10 g (44%).

^{1}H NMR (400 MHz, $CDCl_3$): δ(ppm) 1.12 (3H, d, J = 6.13 Hz, $OCH(CH_3)CH_2N(CH_3)_2$), 2.13 (2H, m, $OCH(CH_3)CH_2N(CH_3)_2$), 2.27 (6H, s, $OCH(CH_3)CH_2N(CH_3)_2$), 3.78 (1H, br m, $OCH(CH_3)CH_2N(CH_3)_2$). ^{13}C NMR (100 MHz, $CDCl_3$): δ(ppm) 24.6 ($OCH(CH_3)CH_2N(CH_3)_2$), 46.1 ($OCH(CH_3)CH_2N(CH_3)_2$), 70.3 ($OCH(CH_3)CH_2N(CH_3)_2$). Calcd for $C_{20}H_{48}CeN_4O_4$: C 43.78, H 8.82, N 10.21; found C 43.96, H 8.76, N 10.07%.

[Ce(dmop)$_4$] ***4*** A solution of $[NH_4]_2[Ce(NO_3)_6]$ (CAN) (1.00 g, 1.82 mmol) in dimethoxyethane (DME) (20 mL) was added at room temperature to a stirred solution of $[NaOBu^t]$ (1.05 g, 10.9 mmol) in DME. After removal of the $NaNO_3$ precipitate, the filtrate was stirred at 0 °C, and a solution of dmopH (1.13 g, 7.30 mmol) in DME (10 mL) was added. The reaction mixture was allowed to warm to room temperature and stirred overnight. Volatiles were removed in vacuo, and the yellow solid residue was extracted with toluene (3 × 50 mL), which was then concentrated to give the product as yellow crystals on cooling to −18 °C. Yield: 437 mg (31.3%).

^{1}H NMR (400 MHz, C_7D_8): δ(ppm) 1.52 (6H, s, $NC(CH_3)_2CH_2$), 1.54 (6H, s, $OC(CH_3)_2C$), 3.82 (2H, s, $NC(CH_3)_2CH_2$). ^{13}C NMR (100 MHz, C_7D_8): δ(ppm) 27.9 ($NC(CH_3)_2CH_2$), 28.0 ($OC(CH_3)_2C$), 77.0 ($NC(CH_3)_2CH_2$), 78.4 ($OC(CH_3)_2C$), 80.6 ($NC(CH_3)_2CH_2$). Calcd for $CeC_{32}H_{56}N_4O_8$: C 50.25, H 7.38, N 7.32; found C 50.07, H 7.49, N 7.19%.

Characterization of [Ce$_2$(dmop)$_6$O] ***5***. $[Ce_2(dmop)_6O]$ was found as the residue after attempts to sublime $[Ce(dmop)_4]$ in vacuo.

^{1}H NMR (400 MHz, C_7D_8): δ(ppm) 1.02 (s), 1.16 (d, J = 3.3 Hz), 1.44 (br s), 1.52 (br m), 1.53 (br s), 1.65 (s), 1.74 (s), 1.78 (s), 1.84 (s), 2.08 (br m), 3.47 (s), 3.57 (s), 3.64 (d, J = 3.3 Hz), 3.79 (br s), 3.82 (br s), 3.90 (br s), 3.92 (br s). ^{13}CNMR (100 MHz, C_7D_8): δ(ppm) 27.6, 30.0, 28.2, 28.4, 28.6, 28.7, 28.8 ($NC(CH_3)_2CH_2$), 30.1, 30.4, 30.8, 31.2, 32.1, 32.2 ($OC(CH_3)_2C$), 66.7, 66.9, 67.3 ($NC(CH_3)_2CH_2$), 77.1, 78.4, 79.4 ($OC(CH_3)_2C$), 80.7, 81.8, 82.5, 82.7 ($NC(CH_3)_2CH_2$), 171.4 ($OC(CH_3)_2C$). Calcd for $Ce_2C_{48}H_{84}N_6O_{13}$: C 46.74, H 6.86, N 6.81; found C 46.89, H 6.92, N 6.85%.

[Ce(dmomp)$_4$] ***6*** was synthesized in the same way as $[Ce(mmp)_4]$ using $[NH_4]_2[Ce(NO_3)_6]$ (532 mg, 0.970 mmol) and $NaOBu^t$ (562 mg, 5.85 mmol). Following the preparation of $[Ce(OBu^t)_4]$, the intermediate Hdmomp (800 mg, 3.90 mmol) in DME (10 mL) was added to the yellow solution with stirring at room temperature. A color change to deep red was seen and after 2 h the volatiles were removed in vacuo to give a powdery amorphous red solid. Yield: 328 mg (35%).

^{1}H NMR (400 MHz, $CDCl_3$): δ(ppm) 0.95 (3H, s, $NC(CH_3)_2CH_2$), 1.21 (3H, s, $NC(CH_3)_2CH_2$), 2.04 (3H, s, $CH_3(C_6H_3O)$), 3.87 (1H, d, J = 7.9 Hz, $NC(CH_3)_2CH_2$), 3.97 [1H, d, J = 7.8 Hz, $NC(CH_3)_2CH_2$), 6.54 [1H, t, C_6H_3), 7.23 (1H, s, C_6H_3), 7.71 (1H, d of d, C_6H_3). ^{13}C NMR (100 MHz, $CDCl_3$): δ(ppm) 15.2 ($CH_3(C_6H_3O)$), 24.6 ($NC(CH_3)_2CH_2$), 27.5 ($NC(CH_3)_2CH_2$), 68.7 ($NC(CH_3)_2CH_2$), 77.6 ($NC(CH_3)_2CH_2$), 116.0 (aromatic), 116.4 (aromatic), 123.9 (aromatic), 126.6 (aromatic), 133.0 (aromatic), 161.8 ($CH_2(C_5H_3CO)$), 165.5 ($CH_3(C_6H_3O)CN$). MS (EI): m/z = 956.3 (M^+); calcd. for $[C_{48}H_{56}CeN_4O_8]^+$, 956.3.

[Ce(mmp)$_2$(dbm)$_2$] ***7***. A solution of Hdbm (dibenzoylmethane) (800 mg, 3.60 mmol) in toluene (20 mL) was added dropwise via canula to a stirred solution of $[Ce(mmp)_4]$ (1.00 g, 1.80 mmol) in toluene (20 mL) at 0 °C. After full addition the reaction was stirred for 1 h at 0 °C and allowed to warm to room temperature for a further 1 h. The volatiles from the deep orange solution were removed in vacuo, and the crude oil recrystallized from toluene to give a low melting point solid at −18 °C. Yield: 447 mg (31.2%).

dx.doi.org/10.1021/ic201593s |*Inorg. Chem.* 2011, 50, 11644–11652

Table 1. Conditions for Thin Film Growth

General Growth Conditions	
solvent	toluene
precursor conc	0.05 M
evaporator temperature	100 °C
reactor pressure	1 mbar
argon flow rate	200 cm^3/min
MOCVD Growth Conditions	
substrate temps	200−600 °C
oxygen flow rate	100 cm^3/min^{-1}
ALD Growth Conditions	
substrate temps	100−350 °C
oxygen source	H_2O: ([Ce(mmp)$_4$], [Ce(dmap)$_4$], [Ce(OC(CH$_3$)$_2$Pr^i])
	O_3: ([Ce(thd)$_4$])
number of cycles	300
pulse sequence (s)	2/2/0.5/3.5
precursor/purge/oxygen source/purge	

^{1}H NMR (400 MHz, d$_8$-thf): δ(ppm) 1.06 (6H, s, C(C***H***$_3$)$_2$), 3.08 (2H, s, C***H***$_2$), 3.28 (3H, s, OC***H***$_3$), 6.85 (1H, s, (C$_6$H$_5$CO)$_2$C***H***), 7.27 (m, aromatic), 7.38 (m, aromatic), 8.10 (m, aromatic). ^{13}C NMR (100 MHz, d$_8$-thf): δ(ppm) 26.8 (OC(***C***H$_3$)$_2$CH$_2$OCH$_3$), 59.2 (OC(CH$_3$)$_2$-CH$_2$O***C***H$_3$), 69.6 (O***C***(CH$_3$)$_2$CH$_2$OCH$_3$), 82.7 (OC(CH$_3$)$_2$***C***H$_2$OCH$_3$), 98.3 ((C$_6$H$_5$CO)$_2$***C***H), 128.8 (aromatic), 129.6 (aromatic), 130.5 (aromatic), 130.6 (aromatic), 131.2 (aromatic), 131.9 (aromatic), 139.8 (aromatic), 185.0 ((C$_6$H$_5$***C***O)$_2$CH). Calcd for $CeC_{40}H_{44}O_8$: C 60.59, H 5.59; found C 60.68, H 5.40%. MS (ASAP): m/z = 793.22 ([M + H]$^+$); calcd for [$CeC_{40}H_{44}O_8$ + H] 793.22.

[Ce(dmap)$_2$(dbm)$_2$] ***8***. A solution of Hdbm (dibenzoylmethane) (433 mg, 1.93 mmol) in toluene (4 mL) was added dropwise via canula to a stirred solution of [Ce(mmp)$_4$] (530 mg, 0.970 mmol) in toluene (20 mL) at 0 °C, and the reaction was stirred for 2 h. Volatiles were removed in vacuo to give the compound as an orange/red oil. Yield: 613 mg (79.9%).

^{1}H NMR (400 MHz, C_7D_8): δ(ppm) 1.08 (3H, d, J = 5.8 Hz, OCH(C***H***$_3$)CH$_2$N(CH$_3$)$_2$), 2.25 [6H, s, OCH(CH$_3$)CH$_2$N(C***H***$_3$)$_2$), 2.44 (1H, d, J = 9.8 Hz, OCH(CH$_3$)C***H***$_2$N(CH$_3$)$_2$), 3.41 [1H, t, J = 11.4 Hz, OCH(CH$_3$)C***H***$_2$N(CH$_3$)$_2$), 5.23 [1H, br m, OC***H***(CH$_3$)CH$_2$N-(CH$_3$)$_2$), 6.43 (1H, s, (C$_6$H$_5$CO)$_2$CH), 7.07 [6H, t, J = 7.5 Hz, aromatic), 7.17 [5H, d, J = 7.1 Hz, aromatic], 7.17 (2H, d, J = 8.0 Hz, aromatic), 7.26 [3H, t, J = 7.1 Hz, aromatic), 7.78 (3H, d, J = 7.5 Hz, aromatic). ^{13}C NMR (100 MHz, $CDCl_3$): δ(ppm): 20.3 (OCH(***C***H$_3$)-CH$_2$N(CH$_3$)$_2$), 46.2 (OCH(CH$_3$)CH$_2$N(***C***H$_3$)$_2$), 71.3 (OCH(CH$_3$)-***C***H$_2$N(CH$_3$)$_2$), 95.7 ((C$_6$H$_5$)$_2$(CO)$_2$***C***H), 124.2 (aromatic), 126.5 (aromatic), 126.8 (aromatic), 127.1 (aromatic), 127.9 (aromatic), 129.3 (aromatic), 136.6 (aromatic), 139.1 (aromatic), 182.9 ((C$_6$H$_5$)$_2$-(***C***O)$_2$CH). Calcd for $C_{40}H_{46}CeN_2O6$: C 60.74, H 5.86, N 3.54; found C 60.64, H 6.03, N 3.46%

[Ce(mmp)$_2$(dmomp)$_2$] ***9***. A solution of dmompH (179 mg, 0.870 mmol) in toluene (10 mL) was added dropwise via canula to a stirred solution of [Ce(mmp)$_4$] (241 mg, 0.870 mmol) in toluene (10 mL) at −83 °C (liquid N_2/ethylacetate). On addition of the ligand a color change from yellow to orange was seen. After stirring for 1 h the volatiles were removed in vacuo to give an orange oil. Yield: 185 mg (56.2%).

^{1}H NMR (400 MHz, C_7D_8): δ(ppm) 1.14 (3H, br, s, NC-(C***H***$_3$)$_2$CH$_2$), 1.31 (6H, s, OC(C***H***$_3$)$_2$CH$_2$OCH$_3$), 1.66 (3H, br s, NC(C***H***$_3$)$_2$CH$_2$), 2.49 (3H, s, C***H***$_3$(C$_6$H$_3$O)), 3.19 (2H, s, OC-(CH$_3$)$_2$C***H***$_2$OCH$_3$), 3.22 (3H, s, OC(CH$_3$)$_2$CH$_2$OC***H***$_3$), 3.56 (2H, s, NC(CH$_3$)$_2$C***H***$_2$), 6.56 (1H, t, J = 7.3 Hz, CH$_3$(C$_6$***H***$_3$O)), 7.22 (1H, d, J = 7.2 Hz, CH$_3$(C$_6$***H***$_3$O)), 7.86 (1H, d, J = 8.0 Hz, CH$_3$(C$_6$***H***$_3$O)). ^{13}C NMR (100 MHz, C_7D_8): δ(ppm) 17.0 (***C***H$_3$(C$_6$H$_3$O)), 28.3 (OC(***C***H$_3$)$_2$CH$_2$OCH$_3$), 29.4 (NC(***C***H$_3$)$_2$CH$_2$), 59.2 (OC(CH$_3$)$_2$-CH$_2$O***C***H$_3$), 68.6 (O***C***(CH$_3$)$_2$CH$_2$OCH$_3$), 78.9 (N***C***(CH$_3$)$_2$CH$_2$), 84.5 (OC(CH$_3$)$_2$***C***H$_2$OCH$_3$), 115.6 (NC(CH$_3$)$_2$***C***H$_2$), 117.0 (CH$_3$(***C***$_6$H$_3$O)), 127.0 (CH$_3$(***C***$_6$H$_3$O)), 128.5 (CH$_3$(***C***$_6$H$_3$O)), 129.3 (CH$_3$(***C***$_6$H$_3$O)), 134.9 (CH$_3$(***C***$_6$H$_3$O)), 166.0 (CH$_3$(***C***$_6$H$_3$O)), 167.1 ((C$_6$H$_3$O)***C***NC-(CH$_3$)$_2$). Calcd for $CeC_{34}H_{50}N_2O_8$: C 54.10, H 6.68, N 3.7; found C 53.86, H 6.45, N 3.56%. MS (EI): m/z = 752.3 ([M − 2H]$^+$), calcd for [$CeC_{34}H_{50}N_2O_8$ − 2H]$^+$ 752.2; MS (CI, NH_3): m/z = 753.3 ([M − H]$^+$), calcd for [$CeC_{34}H_{50}N_2O_8$ − H] 753.2.

Reaction of [Ce(mmp)$_4$] with 2 equiv of Hdmop. A solution of Hdmop (499 mg, 3.17 mmol) in toluene (10 mL) was added dropwise via canula to a stirred solution of [Ce(mmp)$_4$] (877 mg, 1.59 mmol) in toluene (20 mL) at 0 °C, and the reaction was stirred for 2 h. The volatiles were removed in vacuo, and the crude materials recrystallized in toluene to give [Ce$_2$(mmp)$_2$-(dmop)$_4$O] **10** as yellow crystals (253 mg, 19.3% yield).

^{1}H NMR (400 MHz, C_7D_8): δ(ppm) 1.42 (6H, s), 1.48 (24H, m), 1.57 (6H, s), 1.65 (6H s), 1.74 (6H, s), 1.79 (6H, s), 1.96 (6H, s), 3.39 (6H s), 3.34 (2H, d, J = 2.2 Hz), 3.38 (2H, d, J = 2.2 Hz), 3.74 (2H, d, J = 8.1 Hz), 3.76 (2H, d, J = 8.1 Hz), 3.78 (2H, d, J = 8.1 Hz), 3.91 (2H, d, J = 8.1 Hz). Calcd for $Ce_2C_{42}H_{78}O_{13}N_4$: C 44.75, H 6.97, N 4.97; found C 44.60, H 6.84, N 4.90%.

Attempted Synthesis of [Ce(ONep)$_4$]. [Ce(OBu^t)$_4$] was prepared from [NH_4]$_2$[$Ce(NO_3)_6$] (1.00 g, 1.82 mmol) in dimethoxyethane (DME) (20 mL) and NaOBu^t (1.05 g, 10.9 mmol) in DME. After removal of the $NaNO_3$ precipitate, the filtrate was stirred at room temperature and a solution of neopentyl alcohol (642 mg, 7.28 mmol) in toluene (4 mL) was added. The reaction mixture was heated under reflux for 1 h, and then left to cool to room temperature. Volatiles were removed in vacuo and recrystallization of the oil attempted in toluene at −18 °C. Yield of crystalline material = 340 mg. Single crystal X-ray diffraction showed this material to be [Ce$_3$(OBu^t)(ONep)$_9$O] **11**.

Calcd for $Ce_3C_{49}H_{108}O_{11}$: C 45.49, H 8.41%; found C 40.89, H 7.63%. ^{1}H NMR (400 MHz, C_7D_8): δ(ppm) 0.81(13 H, broad s), 3.04 (2H, broad s). ^{13}C NMR (C_7D_8): δ(ppm) 26.7, 27.1.

Crystal Structure Determinations. Crystals were mounted on glass fibers and placed in a cold stream at 100 K. Single crystal X-ray data were collected on a Bruker D8 diffractometer with an APEX CCD detector, and 1.5 kW graphite monochromated Mo radiation. The detector to crystal distance was 5.98 cm. Exposure times of 10 s per frame and scan widths of 0.3° were used throughout the data collections. The frames were integrated with SAINT v7.45a.[14] The structures were solved and refined with X-SEED,[15] a graphical interface to SHELX.[16] Crystal data are summarized in Table 2, and a cif file is available in the Supporting Information.

Thin Film Growth and Characterization. The CeO_2 films were deposited on n-Si(100) wafers. Deposition of the CeO_2 films was performed by liquid-injection ALD or liquid-injection MOCVD using an Aixtron AIX 200FE AVD reactor fitted with a modified liquid-injector system.[17] The delivery of cerium precursor was achieved using a 0.05 M solution of the precursor compound in toluene. Deionized water or ozone (for [Ce(thd)$_4$]) was used as a source of oxygen for ALD growth. Details of the MOCVD and ALD growth conditions are summarized in Table 1.

X-ray diffraction patterns were measured using a Rigaku Miniflex diffractometer using Cu Kα radiation (0.154051 nm, 40 kV, 50 mA) spanning a 2θ range of 20−50° at a scan rate of 0.01°/min.

Raman spectra were acquired using a Jobin-Yvon LabRam HR consisting of a confocal microscope coupled to a single grating spectrometer equipped with a notch filter and a CCD camera detector. The Raman measurements were taken using a confocal aperture of 300 μm to limit the light taken to the center of the microscope lens and hence

Table 2. Crystal Structure and Refinement Data

	[Ce(dmap)$_4$] **3**	[Ce(dmop)$_4$]·C$_7$H$_8$ **4**	[Ce$_2$(mmp)$_2$(dmop)$_4$O]·C$_7$H$_8$ **10**	[Ce$_3$(OBu^t)(ONep)$_9$O] **11**
habit	prism	prism	prism	prism
formula	$C_{20}H_{48}CeN_4O_4$	$C_{39}H_{64}CeN_4O_8$	$C_{49}H_{86}Ce_2N_4O_{13}$	$C_{73}H_{152}Ce_3O_{11}$
formula weight	548.74	857.06	1219.46	1626.31
space group	$P6_122$	$P2_1/c$	$P2_1$	$P\bar{3}c1$
a, Å	9.8993(3)	11.514(5)	10.791(3)	19.0918(17)
b, Å	9.8993(3)	12.546(6)	18.425(5)	19.0918(17)
c, Å	46.8411(16)	29.583(13)	14.533(4)	23.342(2)
α, deg	90.0	90.0	90.0	90.0
β, deg	90.0	96.245(8)	99.530(4)	90.0
γ, deg	120.0	90.0	90.0	120.0
volume, Å^3	3975.3(2)	4248(3)	2849.6(14)	7368.2(11)
Z	6	4	2	4
ρ_{calc}, g/cm	1.375	1.340	1.421	1.466
F_{000}	1716	1792	1256	3408
temp, K	100(2)	100(2)	100(2)	100(2)
$R1$ ($I > 2\sigma(I)$), %	2.4	2.15	3.24	4.74
goodness of fit	1.335	1.069	1.057	0.969

improve the quality of signal achieved. The measurements spanned 150−1500 cm^{-1} with four accumulations and an exposure time of 30 s. All of the spectra were recorded in a backscattering geometry using an incident wavelength of 325 nm from a He−Cd laser.

RESULTS AND DISCUSSION

Choice of Potential Precursor Complexes. Some Ce(III) complexes, for example β-ketoiminates,[18−20] have been used as precursors for CVD of CeO_2. However the synthesis of volatile Ce(III) precursors poses a real challenge: it is difficult to fill the coordination sphere of the large Ce^{3+} ion. Therefore, many Ce(III) complexes with monodentate ligands form dimers or oligomers, and their volatility is consequently reduced. A further potential problem is that many Ce(III) complexes are very prone to at least partial oxidation, making them difficult to obtain and keep in a pure state. We therefore chose to work with Ce(IV): the increased charge and decreased radius of Ce^{4+} compared with Ce^{3+} means that, providing the +4 oxidation state can be stabilized, it should be less difficult to obtain monomeric (and hence potentially more volatile) complexes. There are several well-known Ce(IV) complexes with monodentate alkoxide ligands e.g. [Ce(OBu^t)$_4$], [Ce$_2$(O^{i}Pr)$_8$], and [Ce(OCMe$_2$Pr^i)$_4$]. [Ce(OBu^t)$_4$] and [Ce$_2$(O^{i}Pr)$_8$] are unsuitable as CVD precursors: they are thermally very unstable and readily decompose to form O-bridged clusters with much reduced volatility.[21,22] [Ce(OBu^t)$_4$] is also reported to undergo partial reduction in solution, resulting in the formation of the mixed-valence cluster [Ce$_3$(OBu^t)$_{11}$] which contains two Ce^{4+} and one Ce^{3+}.[23] [Ce(OCMe$_2$Pr^i)$_4$] has been used for MOCVD of CeO_2;[8] however, we found that it has an extremely narrow temperature window for MOCVD (see Figure 9) which seriously limits its use in our reactor system. The thermal instability of [Ce(OBu^t)$_4$] and [Ce$_2$(O^{i}Pr)$_8$] can be attributed to the facile elimination reaction shown in Scheme 1 below (generally referred to by CVD chemists as a "β-hydride" elimination reaction)[24] and formation of a reactive Ce−OH moiety which can then react further to form oxo-bridged species.

Scheme 1. β-Hydride Elimination Reaction of a *tert*-Butoxide Complex

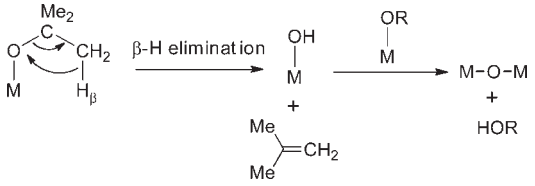

We therefore initially decided to investigate [Ce(ONep)$_4$] (ONep = neopentoxide, OCH$_2$CMe$_3$) which cannot undergo the β-hydride elimination reaction and so should show enhanced stability. However, synthesis of this complex via a salt metathesis reaction of [NH$_4$]$_2$[Ce(NO$_3$)$_6$] with NaONep was unsuccessful, and the alcohol exchange reaction of [Ce(OBu^t)$_4$] with 4 equiv of HONep gave an oily product which crystallized to give [Ce$_3$(μ_3-O)(μ_3-OBu^t)(μ_2-ONep)$_3$(ONep)$_6$] **11** (see Figure 7). The retention of one OBu^t ligand in this complex suggests that the condensation to an oxo-bridged trimer had occurred before the alcohol exchange reaction was complete.

Synthesis of Complexes. *Homoleptic Complexes.* We initially attempted to synthesize new complexes by a salt metathesis reaction between NaOR and ceric ammonium nitrate ([NH$_4$]$_2$[Ce(NO$_3$)$_6$], CAN);[25] however, this method never gave satisfactory yields and frequently gave none of the desired product at all. We therefore used alcohol exchange reactions of [Ce(OBu^t)$_4$], which is readily synthesized from NaOBu^t and [NH$_4$]$_2$[Ce(NO$_3$)$_6$]. [Ce(OBu^t)$_4$] is somewhat fragile in solution, readily decomposing to form [Ce$_3$(μ_3-O)(OBu^t)$_{10}$],[21] and so, we used a simplified synthesis, avoiding the isolation of [Ce(OBu^t)$_4$], as outlined in Scheme 2.

The synthesis of homoleptic complexes by this route was straightforward for all the donor-functionalized alkoxide ligands that we investigated. For example, to synthesize [Ce(mmp)$_4$] **1**, 4 equiv of Hmmp was added at room temperature to the [Ce(OBu^t)$_4$] solution, and after heating to reflux for 2 h, pure product was obtained as yellow crystals in up to 80% yield.

dx.doi.org/10.1021/ic201593s |*Inorg. Chem.* 2011, 50, 11644–11652

Scheme 2. Synthesis of Cerium(IV) Alkoxides via Alcohol Exchange

$$[NH_4]_2[Ce(NO_3)_6] \xrightarrow[THF\ or\ DME]{6NaOBut} [Ce(OBu^t)_4] + 2NH_3 + 6NaNO_3 \xrightarrow{4HOR} [Ce(OR)_4] + 4HOBu^t$$

Similar reaction conditions were used for $[Ce(dmap)_4]$ **3** and $[Ce(dmomp)_4]$ **6**, and these complexes were isolated as crystalline solids. Unfortunately **6** had poor solubility in toluene and decomposed in more polar solvents such as THF or CH_2Cl_2 and was not investigated further. Synthesis of $[Ce(dmop)_4]$ **4** required addition of Hdmop to be performed at 0 °C, followed by reaction at room temperature; otherwise, the product was contaminated with what we believe from analytical data to be $[Ce_2(dmop)_6O]$ **5** (see the Experimental Section).

The reaction of $[Ce(OBu^t)_4]$ with 4 equiv of Hdmae, which is less sterically demanding than Hdmap, was not straightforward: addition of Hdmae at 0 °C followed by stirring at room temperature resulted in incomplete reaction. When the addition of Hdmae was performed at room temperature followed by heating to reflux for 2 h, a yellow oil analyzing as $[Ce(dmae)_4]$ **2** was isolated, but its ^{1}H NMR spectrum was complex (see Figure S2), indicating several different ligand environments. The reaction was not always reproducible, and attempts to sublime **2** in vacuo resulted in decomposition, and elimination of dmaeH. **2** also displayed instability in solution, and we therefore abandoned further investigations of this complex.

Except for $[Ce(dmae)_4]$ **2** and $[Ce(dmomp)_4]$ **6**, all of the homoleptic donor-functionalized alkoxide complexes that we prepared were found by NMR spectroscopy to be indefinitely stable in solution at room temperature: unlike $[Ce(OBu^t)_4]$ and $[Ce_2(OPr^i)_8(HOPr^i)_2]$, there was no evidence of condensation reactions to form oxo-bridged clusters nor was there any evidence of reduction to Ce(III).

Heteroleptic Complexes. We synthesized several heteroleptic complexes with the aim of modifying reactivity and volatility to optimize performance for CVD. Initially we investigated formation of heteroleptic complexes by addition of a mixture of HL proligands to $[Ce(OBu^t)_4]$; however, this method was never successful, generally leading to a mixture of homoleptic complexes. We therefore prepared a series of heteroleptic complexes $[Ce(mmp)_2L_2]$ and $[Ce(dmap)_2L_2]$ by careful addition at low temperature of 2 equiv of HL to $[Ce(mmp)_4]$ or $[Ce(dmap)_4]$, and the complexes were characterized by a combination of elemental analysis, NMR spectroscopy, and mass spectrometry. In the case of L = dmop, we were unable to isolate $[Ce(mmp)_2(dmop)_2]$, but instead the oxo-bridged dimer $[Ce_2(mmp)_2(dmop)_4(\mu_2\text{-}O)]$ **10** was formed and characterized by single crystal X-ray diffraction. Heteroleptic β-diketonate complexes with L = dibenzoylmethanate (dbm) were also prepared by careful reaction of $[Ce(mmp)_4]$ or $[Ce(dmap)_4]$ with 2 equiv of Hdbm (dibenzoylmethane); however, all of our attempts to prepare heteroleptic complexes with thd resulted only in formation of $[Ce(thd)_4]$. The heteroleptic complexes were generally found to be labile in solution: ligand redistribution reactions occurred readily to form mixtures, and so, these complexes were not investigated further as CVD precursors.

Description of Structures. The static structure of an 8-coordinate complex with four bidentate chelating ligands must be chiral unless it has exactly square-prismatic geometry and the ligands contain a plane of symmetry. Although chirality of 6-coordinate tris-chelate complexes has been the subject of many studies, the corresponding phenomenon in 8-coordinate complexes has been relatively unexplored. Here we have an opportunity to examine the structures of three related tetrakis-chelate complexes, including one containing chiral ligands.

[Ce(mmp)$_4$] ***1***. A preliminary report of this complex has already been published;[11] an ORTEP plot of the complex is given in Figure 1 for comparison with other related structures. The Ce atom lies on a crystallographic C_2 axis (see Figure 1b), and it has approximate D_2 symmetry. The room temperature ^{1}H NMR spectrum of this complex (Figure S1 of the Supporting Information) shows that in solution all four mmp ligands are equivalent, and all contain a time-averaged plane of symmetry, which is consistent with D_{2d} symmetry. Rapid inversion of the chelate rings would account for the high-symmetry solution structure; we have been unable to freeze out this process by low temperature ^{1}H NMR spectroscopy.

[Ce(dmap)$_4$] ***3***. The dmap ligand is chiral by virtue of the α-Me substituent, and as we used racemic Hdmap in the preparation of **3**, the formation of diastereomeric mixtures would be possible. In the solid state the complex crystallizes a single

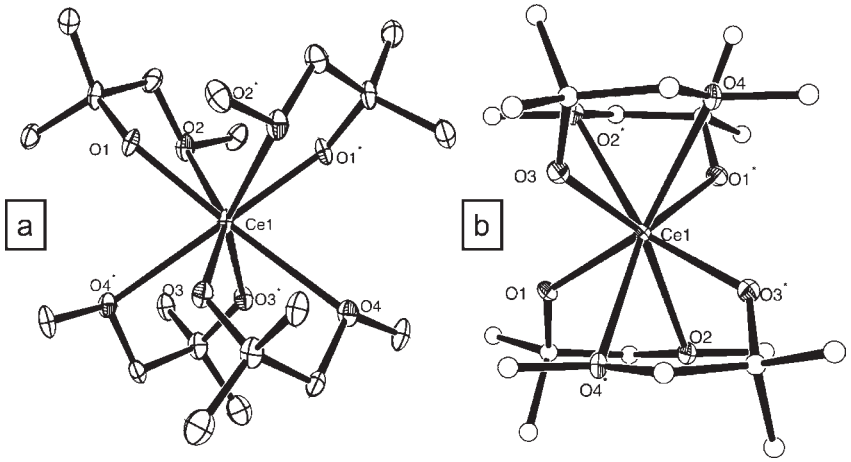

Figure 1. (a) ORTEP plot of $[Ce(mmp)_4]$ **1**. Selected distances (Å) and angles (deg): Ce(1)−O(1), 2.155(5); Ce(1)−O(2), 2.667(4); Ce(1)−O(3), 2.155(4); Ce(1)−O(4), 2.684(4); O(2)−Ce(1)−O(1), 63.99(15); O(4)−Ce(1)−O(3), 63.81(16); O(1)−Ce(1)−O2*, 76.54(14); O(3)−Ce(1)−O(4)*, 76.29(13); O(2)−Ce(1)−O(3), 153.13(16); O(1)−Ce(1)−O(3), 96.09(17); O(1)−Ce(1)−O(4), 153.34(13). O(1), O(1)*, etc. are related by a C_2 rotation. (b) View along crystallographic C_2 axis.

dx.doi.org/10.1021/ic201593s |*Inorg. Chem.* 2011, 50, 11644–11652

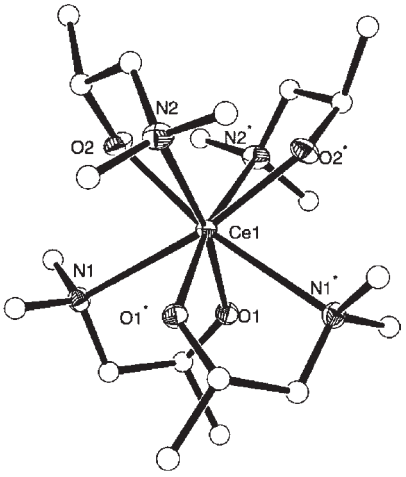

Figure 2. ORTEP plot of [Ce(dmap)$_4$] **3**. Selected distances (Å) and angles (deg) are the following: Ce1−O1, 2.1661(19); Ce1−O2, 2.171(2); Ce1−N1, 2.784(2); Ce1−N2, 2.851(3); O1−Ce1−N1, 64.51(8); O2−Ce1−N2, 64.00(7); O1−Ce1−O1, 94.06(12); N1−Ce1−N1, 122.16(11); O2−Ce1−O2, 97.97(12); N2−Ce1−N2, 120.20(11). O1, O1*; N1, N1*; etc. are related by a C_2 rotation.

diastereomer (Figure 2) containing two *R*-dmap ligands (O2N2 and O2*N2*) and two *S*-dmap ligands (O1N1 and O1*N1*). Similar disastereoselectivity has been observed in [Cu(*R*-dmap)(*S*-dmap)][26] and [Zr_2(O^iPr)$_5$(μ_2-O^iPr)(μ_2-*R*-dmap)(μ_2-*S*-dmap)].[9] However, despite the racemic nature of the ligand combination in **3**, the complex itself is chiral, and it undergoes a spontaneous resolution to crystallize in the rare chiral space group $P6_122$ (143 examples out of a total of 537 899 in the Cambridge Crystallographic Database; January 2011). The donor atoms of the two *S*-ligands (N1, O1, N1*, O1*) are coplanar, as are those of the two *R*-ligands (N2, O2, N2*, O2*).

A simplified view of the complex along the crystallographic C_2 axis (Figure 3) shows how the two parallelograms defined by N1O1N1*O1* and N2O2N2*O2* are twisted by ca. 84° with respect to each other, thus rendering the complex chiral at the Ce atom. The average bite angle of the dmap ligands is 64.25°; the average Ce−O distance is 2.168 Å, and the average Ce−N distance is 2.817 Å.

[Ce(mmp)$_4$] adopts a similarly chiral structure in the solid state, but both enantiomers are present in the unit cell.

The simplicity of the ^{1}H NMR spectrum of [Ce(dmap)$_4$] (Figure S3 of the Supporting Information) indicates that the solution structure consists of a single highly symmetrical diastereomer with all four ligands equivalent, which is a higher symmetry than observed in the solid state. A rotation about the crystallographic C_2 axis of the plane defined by N2O2N2*O2* to give an eclipsed conformation rather than the staggered conformation shown in Figure 3 would introduce a plane of symmetry into the complex. All four ligands are equivalent in the resulting C_{2h} structure. We have not been able to freeze out this process by low temperature NMR spectroscopy.

[Ce(dmop)$_4$] ***4***. An ORTEP plot of **4** is shown in Figure 4. The structure of this 8-coordinate complex in the solid state is very similar to that of [Ce(dmap)$_4$]: the donor atoms (N1, O1, N3, O5) of two of the chelating dmop ligands are close to coplanar, as are those of the other two ligands (N2, O3, N4, O7). As shown in Figure 5, the two planes are twisted by ca. 51° with respect to each other (this is the angle between the two planes defined by

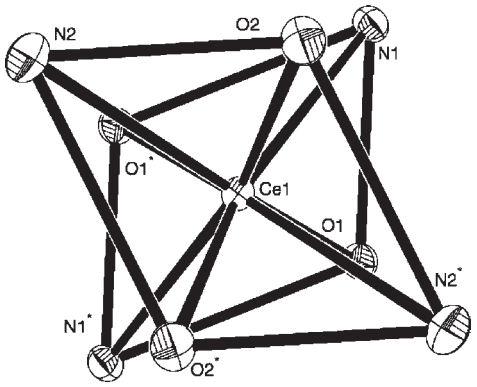

Figure 3. [Ce(dmap)$_4$] **3** viewed along the crystallographic C_2 axis. (C atoms are omitted for clarity).

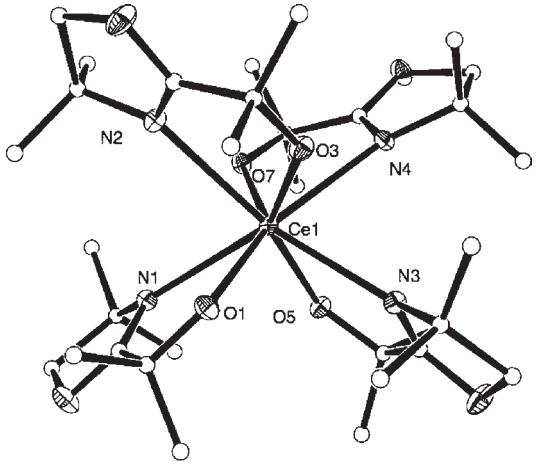

Figure 4. ORTEP plot of [Ce(dmop)$_4$] **4**. Selected distances (Å) and angles (deg): Ce1−O1, 2.1811(11); Ce1−O3, 2.1973(11); Ce1−O5, 2.1758(11); Ce1−O7, 2.1836(11); Ce1−N1, 2.7124(14); Ce1−N2, 2.7246(14); Ce1−N3, 2.6587(13); Ce1−N4, 2.7499(14); O1−Ce1−N1, 63.94(4); O3−Ce1−N2, 64.16(4); O5−Ce1−N3, 64.70(4); O7−Ce1−N4, 64.74(4); N3−Ce1−N1, 122.32(4); N2−Ce1−N4, 106.04(4); O5−Ce1−O1, 99.99(4) ; O7−Ce1−O3, 113.63(4).

O5O1Ce1 and O3O7Ce1), making the complex chiral, but in this case the unit cell has a center of symmetry and so both enantiomeric forms of the complex are present. The average bite angle of the dmop ligands in **4** is 64.38°, very similar to that of the dmap ligands in [Ce(dmap)$_4$]. The average Ce−O distance (2.184 Å) is slightly longer than in [Ce(dmap)$_4$] whereas the average Ce−N distance (2.711 Å) is slightly shorter.

The ^{1}H NMR spectrum of **4** (Figure S5 of the Supporting Information), like those of [Ce(mmp)$_4$] and [Ce(dmap)$_4$], shows a highly symmetrical structure in solution at room temperature: all of the dmop ligands are equivalent, and all have a time-averaged plane of symmetry. A time-averaged plane of symmetry through the dmop ligands can only be achieved through a facile fluxional process at room temperature, resulting in isomerization/racemization of the complex. We have been unable to freeze out this fluxional process by low temperature NMR spectroscopy.

[Ce_2(μ_2-O)(dmop)$_4$(mmp)$_2$] ***10***. This oxo-bridged dimer is chiral with approximate C_2 symmetry, and it crystallizes in the chiral space group $P2_1$. An ORTEP plot of the complex is shown

dx.doi.org/10.1021/ic201593s |*Inorg. Chem.* 2011, 50, 11644–11652

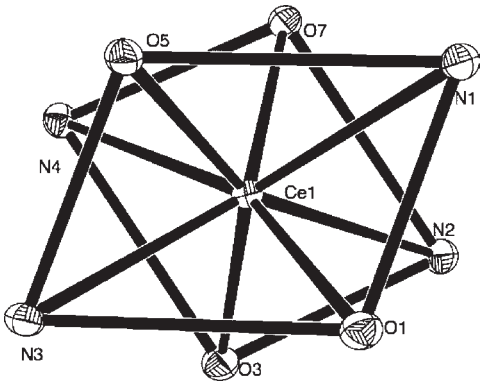

Figure 5. Coordination sphere of one enantiomeric form of $[Ce(dmop)_4]$ (C atoms omitted for clarity).

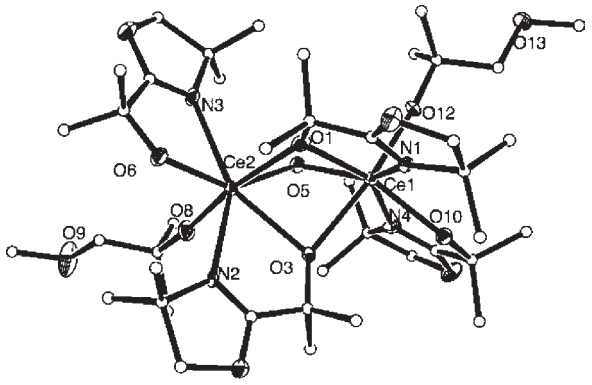

Figure 6. ORTEP plot of $[Ce_2(dmop)_4(mmp)_2(O)]$ **10**. Selected distances (Å) and angles (deg): Ce1−O12, 2.078(5); Ce1−O5, 2.106(5); Ce1−O10, 2.239(5); Ce1−O3, 2.395(5); Ce1−O1, 2.407(5); Ce1−N1, 2.603(5); Ce1−N4, 2.619(6); Ce2−O5, 2.106(4); Ce2−O8, 2.143(5); Ce2−O6, 2.190(5); Ce2−O1, 2.379(5); Ce2−O3, 2.459(5); Ce2−N3, 2.556(6); Ce2−N2, 2.653(5); Ce2−O1−Ce1 89.85(15); Ce1−O3−Ce2 88.25(15); Ce1−O5−Ce2, 106.72(17); O6−Ce2−N3, 65.99(18); O1−Ce1−N1, 63.71(19); O10−Ce1−N4, 64.72(18); O3−Ce2−N2, 62.29(18).

in Figure 6 below, along with selected distances and angles. The two Ce atoms are symmetrically bridged by an oxo ligand and the alkoxide groups of two dmop ligands, and there is an approximate C_2 axis passing through O5 and the midpoint between Ce1 and Ce2. The mmp ligands are both "dangling", as in several other rare earth complexes with this ligand,[27,28] demonstrating again that the OMe group is not a powerful donor. The Ce−O and Ce−N distances for the nonbridging dmop ligands are very similar to those in $[Ce(dmop)_4]$; as expected, the corresponding distances for the bridging dmop ligands are somewhat longer. The Ce−O (alkoxide) distances for the dangling mmp ligands (average 2.110 Å) are very similar to the corresponding distances in the chelating mmp ligands of $[Ce(mmp)_4]$ (average 2.152 Å).

The ^{1}H NMR spectrum of $[Ce_2(\mu_2\text{-}O)(dmop)_4(mmp)_2]$ (Figure S6 of the Supporting Information) shows eight unique Me groups, indicating that the solid state structure is retained in solution.

$[Ce_3(\mu_3\text{-}O)(\mu_3\text{-}OBu^t)(\mu_2\text{-}ONep)_3(ONep)_6]$ ***11***. An ORTEP plot of this complex is shown in Figure 7. The $[M_3(\mu_3\text{-}O)_2]$ moiety is a familiar motif in f-element alkoxide chemistry, and examples are known where both μ_3-O atoms are alkoxides[29] and where one is an alkoxide and one an oxide[30] or hydroxide.[28] **11** is the first fully characterized example with three Ce(IV) atoms and the structure is analogous to that proposed for $[Ce_3O(OBu^t)_{10}]$[21] by analogy with $[U_3O(OBu^t)_{10}]$.[30] The μ_3-O and μ_3-OBu^t ligands are on a crystallographic C_3 axis and so are bonded symmetrically to all three Ce atoms, whereas the μ_2-OBu^t bridges are slightly unsymmetrical with Ce−O distances of 2.331(3) and 2.305(5) Å.

Applications to MOCVD and ALD of CeO_2. *TGA Studies.* Precursors for MOCVD or ALD must generally have some volatility, and TGA can be a useful technique for assessing this. Figure 8 shows TGA traces for $[Ce(mmp)_4]$, $[Ce(dmap)_4]$, $[Ce(dmop)_4]$, and $[Ce(thd)_4]$. $[Ce(mmp)_4]$ sublimed cleanly at atmospheric pressure: sublimation was complete at 250 °C (50% weight loss at 226 °C), leaving a residue of <1.5%. This can be compared with $[Ce(thd)_4]$, probably the most widely used precursor for CVD of CeO_2, (50% weight loss at 275 °C and no residue). None of $[Ce(dmap)_4]$, $[Ce(dmop)_4]$, or $[Ce(dmomp)_4]$ displayed any volatility at atmospheric pressure: all left substantial residues (30% and 26%, respectively), consistent with decomposition to CeO_2. However, we routinely use liquid-injection MOCVD and ALD at reduced pressures, and so, lack of volatility at atmospheric pressure is not necessarily a serious problem. Both $[Ce(mmp)_4]$ and $[Ce(dmap)_4]$ sublimed in vacuo; however, attempts to sublime $[Ce(dmop)_4]$ in vacuo resulted only in sublimation of Hdmop, and a material analyzing as $[Ce_2(dmop)_6(O)]$ was isolated from the residue. $[Ce(dmomp)_4]$ was also involatile in vacuo, so we did not proceed with CVD studies using complexes of dmop or dmomp ligands.

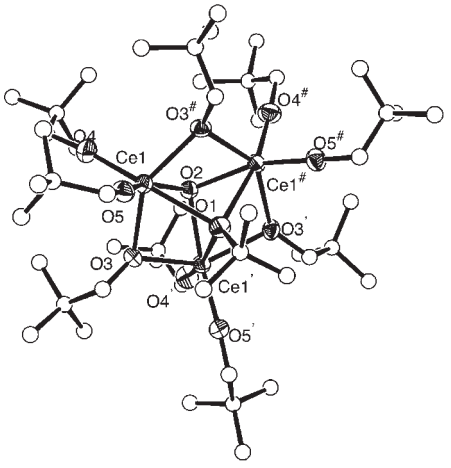

Figure 7. ORTEP plot of $[Ce_3(\mu_3\text{-}O)(\mu_3\text{-}OBu^t)(\mu_2\text{-}ONep)_3(ONep)_6]$ **11**. O3, O3′, O3#, etc. are related by a C_3 rotation. Selected distances (Å) and angles (deg): Ce1−O1, 2.530(4); Ce1−O2, 2.250(2); Ce1−O3, 2.331(3); Ce1−O3#, 2.305(5); Ce1−O4, 2.054(4); Ce1−O5, 2.081(4); Ce1−O1−Ce1#, 87.52(18); Ce1−O2−Ce1#, 102.13(13); Ce1−O3−Ce1#, 98.06(15).

MOCVD. In order to assess the potential of our new precursors, we compared them with the known precursors $[Ce(thd)_4]$ and $[Ce(OCMe_2Pr^i)_4]$.[8] MOCVD growth curves for $[Ce(mmp)_4]$, $[Ce(dmap)_4]$, $[Ce(thd)_4]$, and $[Ce(OCMe_2Pr^i)_4]$ with O_2 as coreactant are shown in Figure 9 below. $[Ce(mmp)_4]$ **1** and $[Ce(dmap)_4]$ **3** both have low temperatures for onset of growth, and although these temperatures were slightly higher than we observed for $[Ce(OCMe_2Pr^i)_4]$, the temperature windows for

dx.doi.org/10.1021/ic201593s |*Inorg. Chem.* 2011, 50, 11644–11652

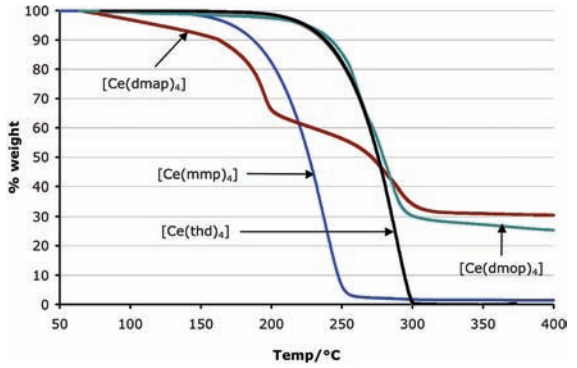

Figure 8. TGA traces for Ce complexes (N_2 atmosphere; heating rate 10 °C/min).

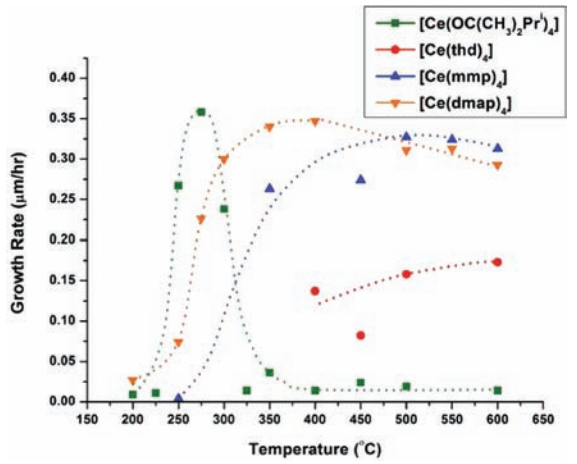

Figure 9. Liquid-injection MOCVD growth curves for $[Ce(thd)_4]$, $[Ce(OCMe_2Pr^i)_4]$, $[Ce(mmp)_4]$, and $[Ce(dmap)_4]$.

MOCVD growth were dramatically wider. We also investigated the possibility of using **1** and **3** as single-source precursors for CeO_2, i.e. in the absence of O_2. Under these conditions, **1** showed growth rates at 350 and 500 °C that were only ca. 10% of those observed in the presence of O_2 whereas **3** showed a growth rate at 400 °C that was ca. 55% of that in the presence of O_2, and therefore, significantly higher than that achieved with $[Ce(thd)_4]$ in the presence of O_2. **3** therefore has potential as a single source precursor for CeO_2. In addition to the obvious growth rate advantages of **1** and **3** when compared with $[Ce(thd)_4]$, we also found that our new alkoxide precursors are much more soluble in toluene than $[Ce(thd)_4]$. We have found that the poor solubility of $[Ce(thd)_4]$ frequently results in experimentally inconvenient injector blockages.

ALD. ALD growth curves for $[Ce(mmp)_4]$ **1** and $[Ce(dmap)_4]$ **3** with H_2O as coreactant are shown in Figure 10, along with data for $[Ce(thd)_4]$ and $[Ce(OCMe_2Pr^i)_4]$ for comparison. It is important to note that due to the weak Brønsted basicity of $[Ce(thd)_4]$, no growth of CeO_2 is observed using H_2O as coreactant, and ozone must be used as the oxygen source. **1** has excellent ALD characteristics: much higher growth rates than for $[Ce(OCMe_2Pr^i)_4]/H_2O$, or $[Ce(thd)_4]/O_3$, and a large window for self-limiting ALD growth from 150 to 350 °C, which is important in order to achieve high reproducibility of film growth and precise control of film thickness by the number of

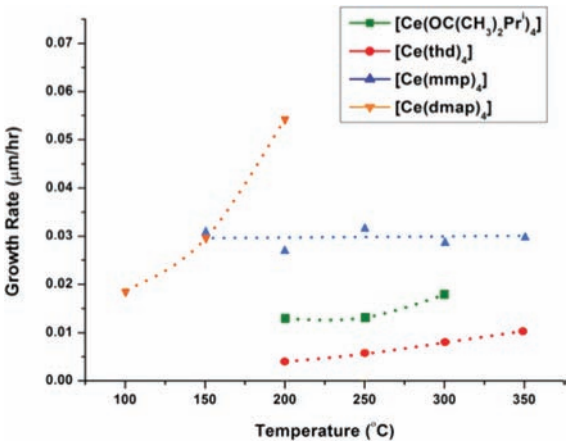

Figure 10. Liquid-injection ALD growth curves for $[Ce(thd)_4]$, $[Ce(OCMe_2Pr^i)_4]$, $[Ce(mmp)_4]$, and $[Ce(dmap)_4]$. The oxygen source was H_2O for $[Ce(OCMe_2Pr^i)_4]$, $[Ce(mmp)_4]$, and $[Ce(dmap)_4]$; it was O_3 for $[Ce(thd)_4]$.

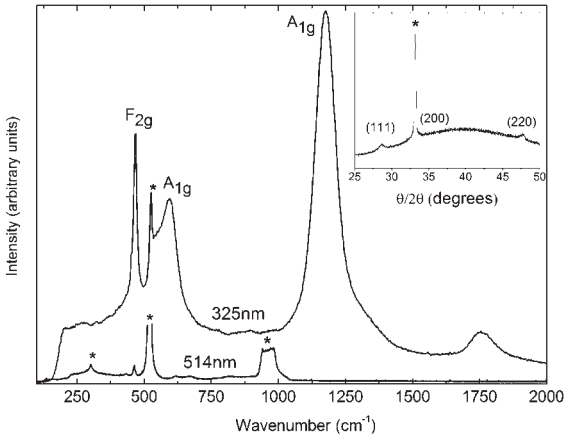

Figure 11. Raman spectra (325 and 514 nm) and XRD (inset) of CeO_2 thin film from $[Ce(dmap)_4]$ (MOCVD, 400 °C, as-grown).

deposition cycles. **3** is less thermally stable than **1** and does not show self-limiting behavior in ALD: there is a large increase in growth rate between 100 and 200 °C indicating thermal decomposition, which is consistent with the onset of MOCVD growth at 200 °C for this precursor.

Characterization of Thin Films. The CeO_2 thin films were characterized by XRD and Raman spectroscopy. Figure 11 shows the 325 and 514 nm Raman spectra for as-grown thin films deposited by MOCVD from $[Ce(dmap)_4]$ at 400 °C. Ceria has one triply degenerate Raman mode at ~465 cm^{-1} with F_{2g} symmetry which is present in traces from both laser sources. The A_{1g} modes seen at ~600 and ~1180 cm^{-1} are second-order modes only picked up by the 325 nm source. Importantly, neither trace shows evidence of the characteristic D and G carbon bands at ~1350 and ~1600 cm^{-1}, respectively, demonstrating minimal carbon inclusion in the films during deposition. These measurements and the XRD plot in the inset show that the films were cubic as grown, and this was found for all the films grown in the 300−600 °C temperature window. Films grown at 350 °C by MOCVD were analyzed by XPS giving the following compositions: $[Ce(mmp)_4]$ precursor Ce, 30.6; O, 62.0; C, 7.4 at %;

dx.doi.org/10.1021/ic201593s |*Inorg. Chem.* 2011, 50, 11644–11652

$[Ce(dmap)_4]$ precursor Ce, 31.8; O, 65.9; C, 2.3 at %. The compositions of the films were derived from the peak areas of the Ce(5d(3/2, 5/2)), O(1s), and C(1s) signals after a nominal ion bombardment to remove adventitious surface contamination. The measurement of carbon content is complicated by the presence of an overlapping Ce XPS peak, and results are are to some extent notional. The XPS data show that the Ce:O ratio is close to 1:2 for films grown from $[Ce(mmp)_4]$ and from $[Ce(dmap)_4]$. Combined with Raman and XRD data this confirms the bulk composition of the films to be CeO_2. A detailed study of materials properties of CeO_2 grown by ALD using $[Ce(mmp)_4]$ is published elsewhere.[31]

CONCLUSIONS

We have prepared a series of homoleptic and heteroleptic complexes of cerium(IV) with donor-functionalized alkoxide ligands and investigated their potential as precursors for the MOCVD and ALD of CeO_2. The homoleptic complexes with mmp, dmap, or dmop ligands show good solution stability with no tendency to decompose either to oxo-bridged structures or to Ce(III) species. The heteroleptic complexes have a tendency to undergo ligand redistribution reactions in solution. The eight-coordinate homoleptic complexes $[Ce(mmp)_4]$ **1** and $[Ce(dmap)_4]$ **3** are both excellent precursors for liquid-injection MOCVD of CeO_2: they exhibit high growth rates and large growth windows, and the thin films show very low carbon contamination, particularly those grown from **3**. **1** is also an excellent precursor for liquid-injection ALD of CeO_2 using H_2O as coreactant, demonstrating a window for self-limiting growth between 150 and 350 °C. Both of these new precursors have significant advantages when compared with the widely used $[Ce(thd)_4]$: higher growth rates in both MOCVD (approximately double) and ALD (approximately 6 times higher), ability to use H_2O instead of ozone as coreactant in ALD, and much better solubility, eliminating problems of injector blockages in the reactor.

ASSOCIATED CONTENT

Supporting Information. NMR spectra of complexes and crystallographic data as a CIF file. This material is available free of charge via the Internet at http://pubs.acs.org.

AUTHOR INFORMATION

Corresponding Author
*E-mail: hca@liv.ac.uk.

ACKNOWLEDGMENT

We thank EPSRC for studentships to J.S.W. and P.J.K., and the EPSRC National Mass Spectrometry Service Centre Swansea for mass spectra.

REFERENCES

(1) Sharma, R. K.; Kumar, A.; Anthony, J. M. *JOM-J. Minerals Met. Mater. Soc.* **2001**, *53*, 53–55.
(2) Chalker, P. R.; Werner, M.; Romani, S.; Potter, R. J.; Black, K.; Aspinall, H. C.; Jones, A. C.; Zhao, C. Z.; Taylor, S.; Heys, P. N. *Appl. Phys. Lett.* **2008**, *93*, 182911.
(3) Bi, L.; Kim, H. S.; Dionne, G. F.; Speakman, S. A.; Bono, D.; Ross, C. A. *J. Appl. Phys.* **2008**, *103*, 07D138.
(4) Jasinski, P.; Suzuki, T.; Anderson, H. U. *Sens. Actuators B-Chem.* **2003**, *95*, 73–77.
(5) Atkinson, A.; Barnett, S.; Gorte, R. J.; Irvine, J. T. S.; McEvoy, A. J.; Mogensen, M.; Singhal, S. C.; Vohs, J. *Nat. Mater.* **2004**, *3*, 17–27.
(6) Jones, A. C.; Aspinall, H. C.; Chalker, P. R.; Potter, R. J.; Manning, T. D.; Loo, Y. F.; O'Kane, R.; Gaskell, J. M.; Smith, L. M. *Chem. Vap. Deposition* **2006**, *12*, 83–98.
(7) Leskela, M.; Ritala, M. *Angew. Chem., Int. Ed.* **2003**, *42*, 5548–5554.
(8) Suh, S.; Guan, J.; Miinea, L. A.; Lehn, J.-S. M.; Hoffman, D. M. *Chem. Mater.* **2004**, *16*, 1667–1673.
(9) Fleeting, K. A.; O'Brien, P.; Jones, A. C.; Otway, D. J.; Andrew, A. J. P.; Williams, D. J. *J. Chem. Soc.-Dalton Trans.* **1999**, 2853–2859.
(10) Loo, Y. F.; O'Kane, R.; Jones, A. C.; Aspinall, H. C.; Potter, R. J.; Chalker, P. R.; Bickley, J. F.; Taylor, S.; Smith, L. M. *Chem. Vap. Deposition* **2005**, *11*, 299–305.
(11) Wrench, J. S.; Black, K.; Aspinall, H. C.; Jones, A. C.; Bacsa, J.; Chalker, P. R.; King, P. J.; Werner, M.; Davies, H. O.; Heys, P. N. *Chem. Vap. Deposition* **2009**, *15*, 259–261.
(12) Pridgen, L. N.; Miller, G. *J. Heterocycl. Chem.* **1983**, *20*, 1223–1230.
(13) Aspinall, H. C.; Beckingham, O.; Farrar, M. D.; Greeves, N.; Thomas, C. D. *Tetrahedron Lett.* **2011**, *52*, 5120–5123.
(14) *SAINT V7.68a*; BRUKER AXS Inc.: WI, USA, 2009.
(15) Barbour, L. J. *J. Supramolec. Chem.* **2001**, *1*, 189–191.
(16) Sheldrake, G. M. *Acta Crystallogr., Sect. A: Found. Crystallogr.* **2008**, *64*, 112–122.
(17) Potter, R. J.; Chalker, P. R.; Manning, T. D.; Aspinall, H. C.; Loo, Y. F.; Jones, A. C.; Smith, L. M.; Critchlow, G. W.; Schumacher, M. *Chem. Vap. Deposition* **2005**, *11*, 159–169.
(18) Belot, J. A.; Wang, A.; McNeely, R. J.; Liable-Sands, L.; Rheingold, A. L.; Marks, T. J. *Chem. Vap. Deposition* **1999**, *5*, 65–69.
(19) Edleman, N. L.; Wang, A.; Belot, J. A.; Metz, A. W.; Babcock, J. R.; Kawaoka, A. M.; Ni, J.; Metz, M. V.; Flaschenriem, C. J.; Stern, C. L.; Liable-Sands, L. M.; Rheingold, A. L.; Markworth, P. R.; Chang, R. P. H.; Chudzik, M. P.; Kannewurf, C. R.; Marks, T. J. *Inorg. Chem.* **2002**, *41*, 5005–5023.
(20) Wang, A.; Belot, J. A.; Marks, T. J.; Markworth, P. R.; Chang, R. P. H.; Chudzik, M. P.; Kannewurf, C. R. *Physica C (Amsterdam)* **1999**, *320*, 154–160.
(21) Evans, W. J.; Deming, T. J.; Olofson, J. M.; Ziller, J. W. *Inorg. Chem.* **1989**, *28*, 4027–4034.
(22) Sirio, C.; HubertPfalzgraf, L. G.; Bois, C. *Polyhedron* **1997**, *16*, 1129–1136.
(23) Arnold, P. L.; Casely, I. J.; Zlatogorsky, S.; Wilson, C. *Helv. Chim. Acta* **2009**, *92*, 2291–2303.
(24) Cameron, M. A.; George, S. M. *Thin Solid Films* **1999**, *348*, 90–98.
(25) Gradeff, P. S.; Schreiber, F. G.; Mauermann, H. *J. Less-Common Met.* **1986**, *126*, 335–338.
(26) Goel, S. C.; Kramer, K. S.; Chiang, M. Y.; Buhro, W. E. *Polyhedron* **1990**, *9*, 611–613.
(27) Anwander, R.; Munck, F. C.; Priermeier, T.; Scherer, W.; Runte, O.; Herrmann, W. A. *Inorg. Chem.* **1997**, *36*, 3545–3552.
(28) Aspinall, H. C.; Bickley, J. F.; Gaskell, J. M.; Jones, A. C.; Labat, G.; Chalker, P. R.; Williams, P. A. *Inorg. Chem.* **2007**, *46*, 5852–5860.
(29) Boyle, T. J.; Ottley, L. A. M. *Chem. Rev.* **2008**, *108*, 1896–1917.
(30) Cotton, F. A.; Marler, D. O.; Schwotzer, W. *Inorg. Chim. Acta* **1984**, *85*, L31–L32.
(31) King, P. J.; Werner, M.; Chalker, P. R.; Jones, A. C.; Aspinall, H. C.; Basca, J.; Wrench, J. S.; Black, K.; Davies, H. O.; Heys, P. N. *Thin Solid Films* **2011**, *519*, 4192–4195.